Site-Selective XANES and EXAFS: A Demonstration with Manganese Mixtures and Mixed-Valence Complexes

Melissa M. Grush,[†] George Christou,[‡]
Keijo Hämäläinen,[§] and Stephen P. Cramer*,[†,||]

Department of Applied Science
University of California, Davis, California 95616
Energy and Environment Division
Lawrence Berkeley Laboratory, Berkeley, California 94720
Department of Chemistry, Indiana University
Bloomington, Indiana 47405
Department of Physics
University of Helsinki, Helsinki, Finland

Received February 15, 1995

This paper presents the first demonstration that chemical shifts in X-ray fluorescence energies can be used to obtain site-selective X-ray absorption spectra. X-ray absorption spectroscopy (XAS) has become a powerful tool for probing both geometric and electronic structure.[1] As commonly practiced, both X-ray absorption near-edge (XANES) and extended X-ray absorption fine structure (EXAFS) techniques measure spectra that average over all species of an element in a sample. In many instances it is desirable to selectively probe different forms of the same element. Such site-selective XAS has previously been accomplished using ion-desorption detection,[2] luminescence detection,[3] X-ray standing waves,[4] and diffraction anomalous fine structure (DAFS).[5] However, all of these methods require specific types of samples, and they are not generally applicable to noncrystalline bulk materials.

Chemical shifts in X-ray emission have been known for many years.[6] More recently, the line sharpening[7a] and spin selectivity[7b,8] gained from high-resolution fluorescence excitation spectroscopy have become appreciated.[9] We have shown that both the energy and shape of Mn Kβ emission change with oxidation and spin state.[8] This suggests that, by picking the appropriate detection energy, it should be possible to selectively probe the absorption spectrum of a particular oxidation state of Mn in a mixed-valence complex. For mixed-valence Mn systems such as batteries[10] and metalloprotein clusters[11] site-selective XAS of Mn(II), Mn(III), and Mn(IV) sites would have many advantages. In this paper, site-selective XANES and EXAFS using high-resolution fluorescence detection are demonstrated for a physical mixture of MnF_2 and $BaMn_8O_{16}{\cdot}2H_2O$ and for a $Mn^{II}Mn^{III}_2$ mixed-valence complex, $Mn_3O(O_2CPh)_6(py)_2(H_2O)$.

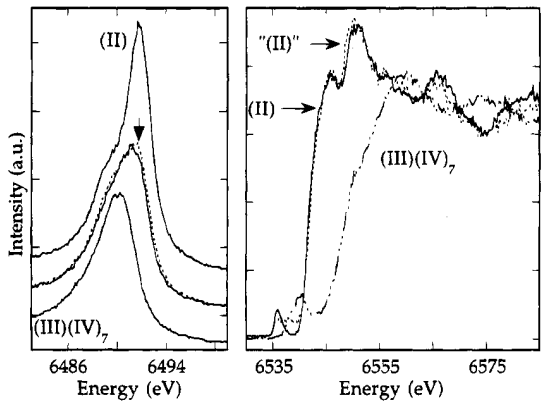

Figure 1. Mn Kβ emission spectra and site-selective XANES. Left: Kβ emission spectra of MnF_2 (top, (II)), $BaMn_8O_{16}{\cdot}2H_2O$ (bottom, (III)-$(IV)_7$), a physical mixture consisting of equal amounts of Mn from both components (middle, —), and the average of the pure component spectra (middle, •••); the energy monitored for probing predominately Mn(II) species in the physical mixture is indicated (arrow). Right: XANES spectra obtained from MnF_2 (—, (II)), $BaMn_8O_{16}{\cdot}2H_2O$ (— • • • —, (III)$(IV)_7$), and the physical mixture monitored at 6491.4 eV (• • •, "(II)").

The Kβ emission spectra of $Mn^{II}F_2$, $BaMn^{III}Mn^{IV}{}_7O_{16}{\cdot}2H_2O$, and their physical mixture are presented in Figure 1.[12] As has been observed before,[8] the Kβ emission peaks at higher energy for lower oxidation states. The physical mixture spectrum is nicely simulated by the average of the two component spectra, as is expected. On the basis of these emission results, the fluorescence analyzer was set at an energy selective for Mn(II) (6491.4 eV), and the excitation energy was scanned. A

[†] University of California.
[‡] Indiana University.
[§] University of Helsinki.
[||] Lawrence Berkeley Laboratory.

(1) *X-ray Absorption: Principles, Applications, Techniques of EXAFS, SEXAFS and XANES*; Konigsberger, D. C., Prins, R., Eds.; Wiley & Sons: New York, 1988.
(2) Jaeger, R.; Stöhr, J. *Phys. Rev. Lett.* **1980**, *45*, 1870−1873.
(3) (a) Goulon, J.; Tola, P.; Brochon, J. C.; Lemonnier, M.; Dexpert-Ghys, J.; Guilard, R. *EXAFS and Near Edge Structure III*; Hodgson, K. O., Hedman, B., Penner-Hahn, J. E., Eds.; Springer-Verlag: Berlin, 1984; pp 490−495. (b) Dexpert-Ghys, J.; Piriou, B.; Jacquetfrancillon, N.; Sombret, C. *J. Non-Cryst. Solids* **1990**, *125*, 117−128.
(4) (a) Yokoyama, T.; Takata, Y.; Yoshiki, M.; Ohta, T.; Funabashi, M.; Kitajima, Y.; Kuroda, H. *Jpn. J. Appl. Phys.* **1989**, *28*, L1637−L1640. (b) Malgrange, C.; Ferret, D. *Nucl. Instrum. Methods Phys. Res. Sect. A* **1992**, *314*, 285−296.
(5) (a) Sorensen, L. B.; Cross, J. O.; Newville, M.; Ravel, B.; Rehr, J. J.; Stragier, H.; Bouldin, C. E.; Woicik, J. C. *Resonant Anomalous X-ray Scattering*; Materlik, G., Sparks, C. J., Fischer, K., Eds.; Elsevier Science: Amsterdam, 1994; pp 389−420. (b) Pickering, I. J.; Sansone, M.; Marsch, J.; George, G. N. *Jpn. J. Appl. Phys.* **1993**, *32*, 206−208.
(6) Ekstig, B.; Källne, E.; Noreland, E.; Manne, R. *Phys. Scr.* **1970**, *2*, 38−44.
(7) (a) Hämäläinen, K.; Siddons, D. P.; Hastings, J. B.; Berman, L. E. *Phys. Rev. Lett.* **1991**, *67*, 2850−2853. (b) Hämäläinen, K.; Kao, C.-C.; Hastings, J. B.; Siddons, D. P.; Berman, L. E.; Stojanoff, V.; Cramer, S. P. *Phys. Rev. B* **1992**, *46*, 14274−14277.
(8) Peng, G.; deGroot, F. M. F.; Hämäläinen, K.; Moore, J. A.; Wang, X.; Grush, M. M.; Hastings, J. B.; Siddons, D. P.; Armstrong, W. H.; Mullins, O. C.; Cramer, S. P. *J. Am. Chem. Soc.* **1994**, *116*, 2914−2920.
(9) Hämäläinen, K.; Siddons, D. P.; Berman, L. E.; Kao, C.-C.; Hastings, J. B. *Resonant Anomalous X-ray Scattering*; Materlik, G., Sparks, C. J., Fischer, K., Eds.; Elsevier Science: Amsterdam, 1994; pp 485−493.
(10) (a) Thackeray, M. M.; Roussouw, M. H.; de Kock, A.; de la Harpe, A. P.; Gummow, R. J.; Pearce, K.; Liles, D. C. *J. Power Sources* **1993**, *43-44*, 289−300. (b) Tarascon, J. M.; Guyomard, D. *Electrochim. Acta* **1993**, *38*, 1221−1231.
(11) Wieghardt, K. *Angew. Chem.* **1989**, *28*, 1153−1172.
(12) Mn site-selective spectra were recorded on NSLS beamline X25[13] using a Si(220) excitation monochromator and a spherically bent Si(440) fluorescence analyzer[14] which has a resolution of ~0.3 eV. The trimer emission spectra were measured on beamline 6-2[15] at SSRL with a Si(111) excitation monochromator and the same fluorescence analyzer. Conventional Mn K-edge X-ray absorption spectra were recorded on Exxon beamline X10C[16] at the NSLS using a Si(220) monochromator. Samples were diluted with BN or sucrose to a concentration of 10% Mn (w/w). The physical mixture consisted of equal amounts of Mn from MnF_2 and $BaMn_8O_{16}{\cdot}2H_2O$ with a total Mn concentration of 10% Mn (w/w). The EXAFS were measured at low temperatures (~77 K); all other spectra were recorded at room temperature. The physical mixture emission spectra were calibrated using 6491.7 eV for the main Kβ peak of MnF_2 as a reference; excitation spectra used either 6543.33 eV for the $KMnO_4$ pre-edge or 6539.0 eV for the first derivative peak of a Mn foil. The EXAFS spectra were smoothed over a k-range of 0.1 or 0.3 $Å^{-1}$ for the transmission and site-selective data, respectively. The Mn trimer emission spectra were normalized to unit intensity at the Kβ peak.
(13) Berman, L. E.; Hastings, J. B.; Oversluizen, T.; Woodle, M. *Rev. Sci. Instrum.* **1992**, *63*, 428−432.
(14) Stojanoff, V.; Hämäläinen, K.; Siddons, D. P.; Hastings, J. B.; Berman, L. E.; Cramer, S. P.; Smith, G. *Rev. Sci. Instrum.* **1992**, *63*, 11255−1127.
(15) Hoyer, E.; Bahr, C.; Chan, T.; Chin, J.; Elioff, T.; Halbach, K.; Harnett, G.; Humphries, D.; Hunt, D.; Kim, K.-J.; Lauritzen, T.; Lindel, D.; Shirley, D.; Tafelski, R.; Thompson, A.; Cramer, S.; Eisenberger, P.; Hewitt, R.; Stöhr, J.; Boyce, R.; Brown, G.; Golde, A.; Gould, R.; Hower, N.; Lindau, I.; Winick, H.; Yang, J.; Harris, J.; Scott, B. *Nucl. Instrum. Methods Phys. Res.* **1983**, *208*, 117−125.
(16) Sansone, M.; Via, G.; George, G. N.; Meitzner, G.; Hewitt, R. *X-ray Absorption Fine Structure*; Hasnain, S. S., Ed.; Ellis Horwood Ltd.: W. Sussex, England, 1991; pp 656−658.

0002-7863/95/1517-5895$09.00/0

spectrum selective for the Mn(II) component of the physical mixture was obtained, as shown in Figure 1. In the region above 6540 eV, the site-selective XANES using 6491.4 eV detection is almost identical to that of the pure MnF_2. Some differences occur in the 1s → 3d region which may be due to contamination by fluorescence from the $BaMn_8O_{16}{\cdot}2H_2O$ and resonant Raman scattering.[17]

To demonstrate that site selectivity can be obtained for EXAFS of mixed-valence complexes, we show the transmission, emission, and excitation spectra of $Mn_3O(O_2CPh)_6(py)_2(H_2O)$ (Figure 2). This trinuclear mixed-valence system has a single trapped-valence Mn(II) center with a different local structure from the two Mn(III) ions.[18] The Mn(II)−Mn(III) distances are 3.36 ± 0.02 Å while the Mn(III)−Mn(III) distance is 3.21 Å. Thus, from the Mn(II) perspective, the Mn−Mn interactions are homogeneous, while the Mn(III) sites see a more disordered environment with two different Mn−Mn distances, resulting in weaker Mn−Mn EXAFS.

The Kβ emission spectrum of $Mn_3O(O_2CPh)_6(py)_2(H_2O)$ is nicely simulated by the weighted average of Mn^{II}_3 and Mn^{III}_3 component spectra (Figure 2). A good fit[19,20] to the transmission data was obtained using either two Mn−Mn interactions at 3.32 Å or $^2/_3$ Mn−Mn at 3.22 Å and $^4/_3$ at 3.37 Å, as well as Mn−O components at 1.85 and 2.13 Å (Figure 2 and supplementary material).

We selectively probed the EXAFS of the Mn(II) and Mn(III) species by monitoring the Kβ fluorescence at 6492.6 and 6488.9 eV, respectively. The site-selective EXAFS oscillations are clearly different from each other (Figure 2). Although they are similar at low k to the transmission spectrum, at high k they show stronger and sharper oscillations. The Fourier transform of the Mn(II) spectrum, which reflects two Mn−Mn interactions at 3.36 Å, shows a clear peak for this interaction, while the transmission and Mn(III)-selective spectra show much broader structure in this region.

Simulations of the smoothed site-selective EXAFS[19,20] required two Mn−O components and at least one Mn−Mn component (Figure 2). Shells of O and C at 3.0 and 3.4 Å also contribute and complicate the analysis. The Mn(II)-selective data was best fitted to a homogeneous Mn−Mn component at 3.36 Å ($R_{crystal}$ = 3.36 Å). For the Mn(III)-selective measurement, the emission from Mn(III) always overlaps that from Mn(II), and the selectivity is lower. Nevertheless, spectra taken using 6488.9 eV detection predominately probe the Mn(III) sites. Fitting with a single Mn−Mn interaction gave an average distance of 3.29 Å ($R_{crystal\text{-}av}$ = 3.29 Å). A slightly better fit was obtained when the Mn(III)−Mn interaction was split into two components at 3.22 Å ($R_{crystal}$ = 3.21 Å) and 3.34 Å ($R_{crystal}$ = 3.36 Å). In the future, better statistics and a wider range of data will certainly allow better discrimination between different models.

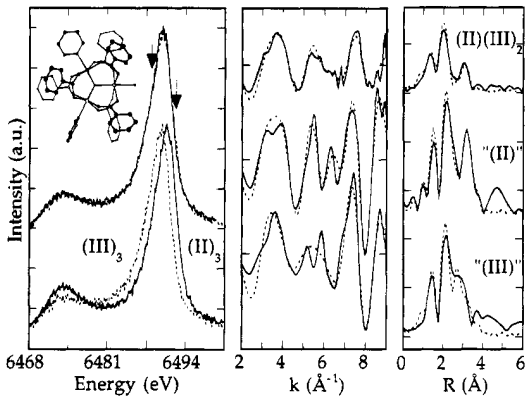

Figure 2. Spectra of $Mn_3O(O_2CPh)_6(py)_2(H_2O)$. Left: Mn Kβ spectrum of $Mn_3O(O_2CPh)_6(py)_2(H_2O)$ (top, —); the energies monitored for probing predominately Mn(III) and Mn(II) species, respectively, are indicated (arrows). Shown below for comparison are the Kβ emission spectra of $Mn(II)_3(O_2CPh)_6(bpy)_2$ (—, $(II)_3$) and $[Mn(III)_3O(O_2CMe)_6(py)_3](ClO_4)$ (•••, $(III)_3$). Also shown is the weighted average of the $Mn(II)_3$ and $Mn(III)_3$ spectra (top, •••). Left inset: Model of $Mn_3O(O_2CPh)_6(py)_2(H_2O)$, shown without the H atoms. Middle: EXAFS data (—) and simulation using one Mn−Mn distance (•••) for $Mn_3O(O_2CPh)_6(py)_2(H_2O)$, monitored by transmission (top); and site-selective EXAFS using 6492.6 eV detection (middle) and using 6488.9 eV detection (bottom). Right: Fourier transform of the EXAFS data (—) and simulation using one Mn−Mn distance (•••) for transmission (top, $(II)(III)_2$); 6492.6 eV detection (middle, "(II)"); and 6488.9 eV detection (bottom, "(III)"). The Fourier transforms have been phase corrected for Mn.

In summary, we have demonstrated the feasibility of site-selective XANES and EXAFS using high-resolution fluorescence detection. There are many cases where fluorescence lines change with chemical environment; hence this method of site-selective XAS should have broad applicability. Useful chemical shifts in emission spectra are known for heavier metals such as the rare earths,[6] for high-spin vs low-spin Fe,[21] for different oxidation states of sulfur,[22] and even for light atoms such as carbon.[23] The main obstacle at the moment is signal-to-noise, but with new high-brightness synchrotron radiation sources[24] and a larger collection solid angle, site-selective XAS using high-resolution fluorescence detection should become a more common and valuable technique.

Acknowledgment. We thank L. Berman, M. Sansone, A. G. Froeschner, C. R. Randall, B. J. Weiss, X. Wang, D. Le, and J. A. Moore for experimental assistance; J. H. Christiansen and M. J. Latimer for helpful scientific discussions; M. W. Wemple for synthesizing the Mn trimers; and A. Campbell for providing the $BaMn_8O_{16}{\cdot}2H_2O$. This research was supported by the National Institutes of Health (GM 48145 and GM 39083), the ACS Petroleum Research Fund (25912-AC3), and the U.S. Department of Energy, Office of Health and Environmental Research. The National Synchrotron Light Source and the Stanford Synchrotron Radiation Lab are supported by the U.S. Department of Energy, Office of Basic Energy Sciences.

Supplementary Material Available: A table of curve-fitting results for the series of simulations on $Mn_3O(O_2CPh)_6(py)_2(H_2O)$ spectra (3 pages). This material is contained in many libraries on microfiche, immediately follows this article in the microfilm version of the journal, can be ordered from the ACS, and can be downloaded from the Internet; see any current masthead page for ordering information and Internet access instructions.

JA950528H

(17) deGroot, F. M. F.; Pizzini, S.; Fontaine, A.; Hämäläinen, K.; Kao, C.-C.; Hastings, J. B. *Phys. Rev. B: Condens. Matter* **1995**, *51*, 1045−1052.

(18) Vincent, J. B.; Chang, H.-R.; Folting, K.; Huffman, J. C.; Christou, G.; Hendrickson, D. N. *J. Am. Chem. Soc.* **1987**, *109*, 5703−5711.

(19) McKale, A. G.; Knapp, G. S.; Chan, S.-K. *Phys. Rev. B* **1986**, *33*, 841−846.

(20) The distances reported here are from fits with coordination numbers fixed at values obtained from the crystal structure[18] and with individual ΔE_0 values held constant at −10 eV. An exception was made for the two short-distance oxygen shells, where the sum of the coordination numbers was fixed, and for the Mn−C interaction, where the coordination number was floated. Additional fits are presented in the supplementary material.

(21) Peng, G.; Wang, X.; Randall, C. R.; Moore, J. A.; Cramer, S. P. *Appl. Phys. Lett.* **1994**, *65*, 2527−2529.

(22) Nilar, S. H.; Zerner, M. C.; Manne, R. *Chem. Phys. Lett.* **1990**, *168*, 260−264.

(23) Skytt, P.; Glans, P.; Mancini, D. C.; Guo, J.-H.; Wassdahl, N.; Nördgren, J. *Phys. Rev. B* **1994**, *50*, 10457−10461.

(24) Margaritondo, G. *Acta Phys. Polon., A* **1994**, *86*, 705−712.